Report

Current Biology

Alternative Splicing Generates a MONOPTEROS Isoform Required for Ovule Development

Highlights

- In ovules, MP localizes and activates its targets in cells with auxin minima
- The MP11ir splicing variant seems to function independently of the AUX/IAAs
- Canonical MP and MP11ir complement *mp* mutants during reproductive development

Authors

Mara Cucinotta, Alex Cavalleri, Andrea Guazzotti, ..., Dolf Weijers, Martin M. Kater, Lucia Colombo

Correspondence

lucia.colombo@unimi.it

In Brief

Cucinotta et al. report that MONOPTEROS in ovules is a transcriptional activator in auxin minima regions. This auxin response factor is functioning independently of auxin regulation during reproductive development as evidenced by the observation that an alternative splicing isoform, uncoupled from auxin regulation, was able to rescue *mp* mutants.

Cucinotta et al., 2021, Current Biology *31*, 1–8
February 22, 2021
https://doi.org/10.1016/j.cub.2020.11.026

CellPress

Current Biology

CellPress
OPEN ACCESS

Report

Alternative Splicing Generates a MONOPTEROS Isoform Required for Ovule Development

Mara Cucinotta,[1,4] Alex Cavalleri,[1,4] Andrea Guazzotti,[1] Chiara Astori,[1] Silvia Manrique,[1] Aureliano Bombarely,[1] Stefania Oliveto,[1,2] Stefano Biffo,[1,2] Dolf Weijers,[3] Martin M. Kater,[1] and Lucia Colombo[1,5,*]

[1]Dipartimento di BioScienze, Università degli Studi di Milano, Via Celoria 26, 20133 Milano, Italy
[2]INGM, National Institute of Molecular Genetics "Romeo ed Enrica Invernizzi," 20122 Milano, Italy
[3]Laboratory of Biochemistry, Wageningen University, Dreijenlaan 3, 6703 HA Wageningen, the Netherlands
[4]These authors contributed equally
[5]Lead Contact
*Correspondence: lucia.colombo@unimi.it
https://doi.org/10.1016/j.cub.2020.11.026

SUMMARY

The plant hormone auxin is a fundamental regulator of organ patterning and development that regulates gene expression via the canonical AUXIN RESPONSE FACTOR (ARF) and AUXIN/INDOLE-3-ACETIC ACID (Aux/IAA) combinatorial system. ARF and Aux/IAA factors interact, but at high auxin concentrations, the Aux/IAA transcriptional repressor is degraded, allowing ARF-containing complexes to activate gene expression. ARF5/MONOPTEROS (MP) is an important integrator of auxin signaling in *Arabidopsis* development and activates gene transcription in cells with elevated auxin levels. Here, we show that in ovules, MP is expressed in cells with low levels of auxin and can activate the expression of direct target genes. We identified and characterized a splice variant of *MP* that encodes a biologically functional isoform that lacks the Aux/IAA interaction domain. This *MP11ir* isoform was able to complement inflorescence, floral, and ovule developmental defects in *mp* mutants, suggesting that it was fully functional. Our findings describe a novel scenario in which *ARF* post-transcriptional regulation controls the formation of an isoform that can function as a transcriptional activator in regions of subthreshold auxin concentration.

INTRODUCTION

Developmental processes in plants require auxin. The auxin signaling pathway is primarily mediated by the interplay between AUXIN RESPONSE FACTOR (ARF) and AUXIN/INDOLE-3-ACETIC ACID (Aux/IAA) proteins.[1,2] At subthreshold auxin concentrations, Aux/IAA repressor proteins bind to ARF transcription factors, thereby repressing the expression of ARF downstream target genes.[3,4] Similar to other canonical ARFs, ARF5/MONOPTEROS (MP), contains three domains: a B3 DNA-binding domain (DBD), a middle region (MR), and a carboxy-terminal domain (CTD) that is required for dimerization with Aux/IAA proteins, such as IAA12/BODENLOS (BDL).[5] It has been proposed that at above threshold auxin levels, MP activates transcription of its targets by recruiting the SWI/SNF chromatin remodelling complex, while at subthreshold auxin concentrations, it is bound by BDL that recruits the TPL/HDA19 co-repressor/histone deacetylase complex to repress transcription.[6]

MONOPTEROS and its many of its identified downstream targets are involved in diverse developmental processes, including embryo development, primary and lateral root formation, vasculature patterning, shoot apical meristem maintenance and floral and ovule initiation.[7–14] This work focuses on a deeper characterization of the expression pattern of MP and its direct targets during ovule development. The results allowed us to hypothesize the existence of non-canonical MP activity that is capable of activating target genes in cells with low levels of auxin. Indeed, we show that alternative splicing (AS) can generate a functional MP isoform that lacks the Aux/IAA dimerization domain, which implies that this isoform regulates transcription in an auxin-independent manner. Our findings suggest an alternative scenario to the classical paradigm of how MP, and potentially other activating ARFs, can be controlled for appropriate target gene regulation.

RESULTS AND DISCUSSION

MP and Its Targets Are Expressed in Regions of Auxin Minima in Ovules

In seed plants, the ovule gives rise to and contains the female gametophyte for the purpose of fertilization. Ovule primordia contain three distinct regions: a proximal region from which the funiculus differentiates, a chalaza that will form the integuments, and the nucellus, from which the megaspore mother cell develops. *In situ* hybridization experiments showed that *MP* was expressed in the proximal region and especially in the chalaza (Figure 1A). At later developmental stages, *MP* expression was limited to the boundary region between the chalaza and the nucellus (Figures 1B and 1C). The expression profile of a functional MP-GFP fusion, encoded by *pMP:MP-GFP*,[15] displayed the same expression pattern (Figures 1D and 1F).

To investigate auxin response in these tissues, we took advantage of the auxin response reporters *DR5v2:ntdTomato*

Please cite this article in press as: Cucinotta et al., Alternative Splicing Generates a MONOPTEROS Isoform Required for Ovule Development, Current Biology (2020), https://doi.org/10.1016/j.cub.2020.11.026

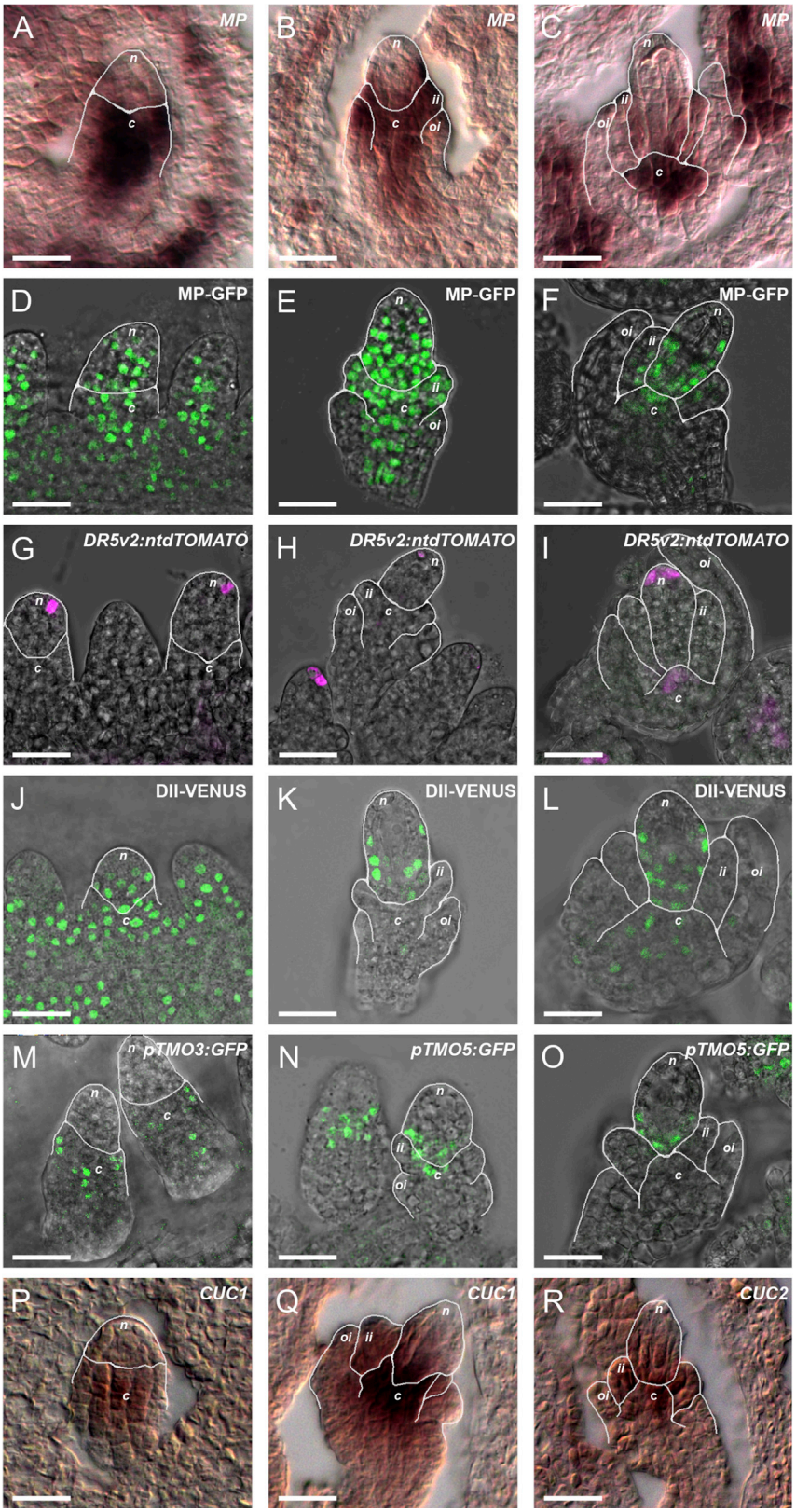

Figure 1. During Ovule Development, *MP* Transcripts, MP Protein, and Direct MP Targets Are Expressed in Regions Characterized by a Low Auxin Response

(A–C) *MP* expression detected by *in situ* hybridization, (D–F) expression of *pMP:MP-GFP,* (G–I) *DR5v2:ntdTomato* and (J–L) *DII-VENUS* in three sequential developmental stages from ovule primordium formation to functional megaspore formation.

(M) *pTMO3:GFP*, (N) and (O) *pTMO5:GFP*, and (P–R) *in situ* hybridization of *CUC1* and *CUC2* transcripts in ovules at megasporogenesis stages. The boundaries between the different ovule structures (n: nucellus; c: chalaza; ii: inner-integument; oi: outer-integument) are outlined in white. Scale bar, 20 μm.

Please cite this article in press as: Cucinotta et al., Alternative Splicing Generates a MONOPTEROS Isoform Required for Ovule Development, Current Biology (2020), https://doi.org/10.1016/j.cub.2020.11.026

CellPress
OPEN ACCESS

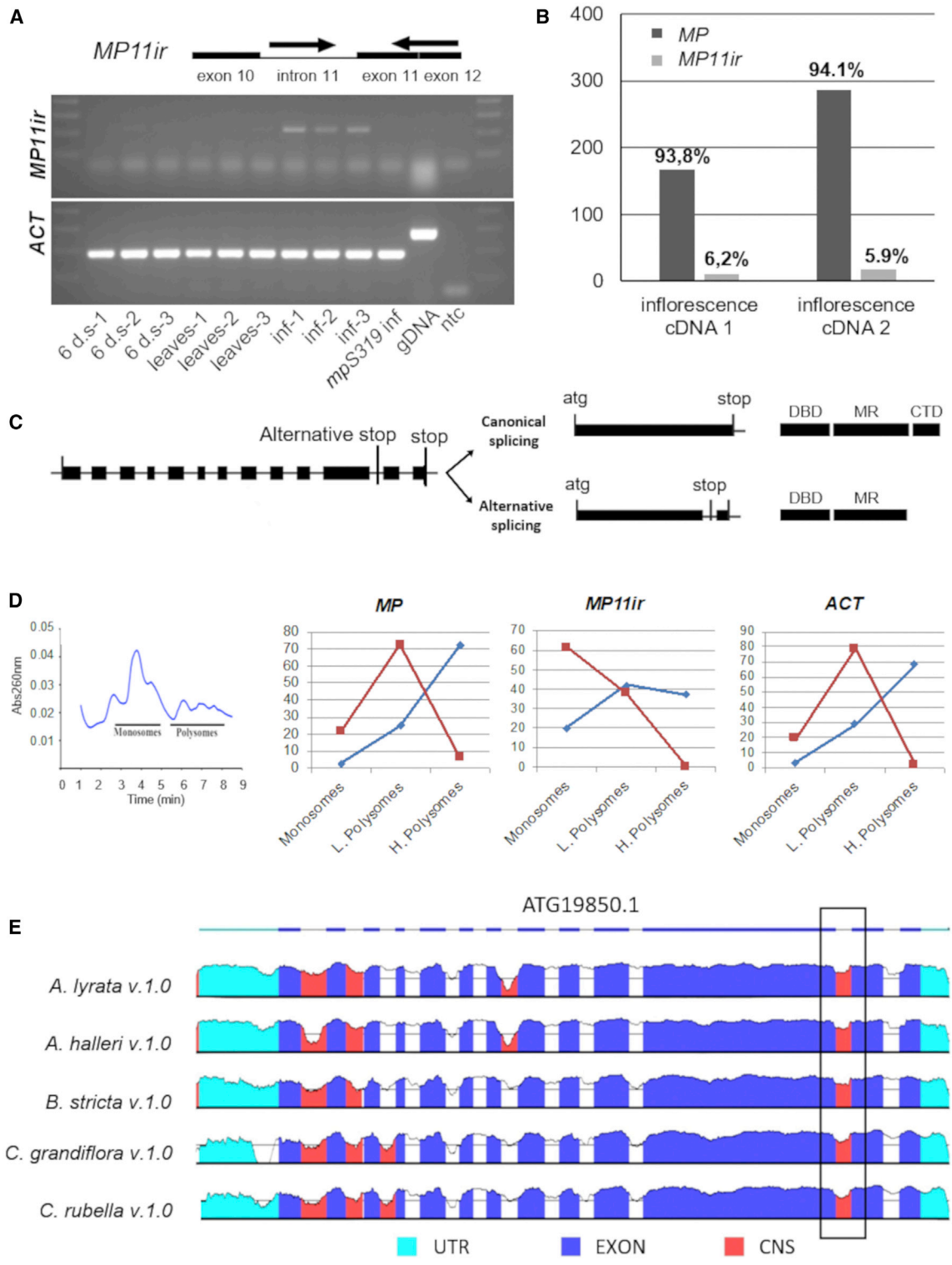

Figure 2. Detection of Alternative Splicing of *MP*

(A) Schematic structure of the *MP* locus showing the position of primers against the canonical cDNA and *MP11ir* cDNA *MP* genomic sequence used to detect alternative spliced isoforms. The forward primer anneals to intron 11, and the reverse primer to the exon 11–exon 12 junction. Correct annealing of both primers only occurs for *MP11ir*, leading to the amplification of a 239-bp fragment. The cDNA quality was tested with *ACTIN 10*.

(B) Quantitative expression data for canonical *MP* and the *MP11ir* alternative isoform by ddPCR.

(C) Intron 11 introduces a premature stop codon into the *MP* ORF, resulting in the translation of a truncated protein that lacks the CTD domain.

(legend continued on next page)

Please cite this article in press as: Cucinotta et al., Alternative Splicing Generates a MONOPTEROS Isoform Required for Ovule Development, Current Biology (2020), https://doi.org/10.1016/j.cub.2020.11.026

and DII-VENUS.[16,17] As already described for the classical *DR5* reporter,[10] *DR5v2* showed a peak of auxin response in a few epidermal cells at the tip of the nucellus (Figure 1G–1I). By contrast, DII-VENUS marked cells with low auxin levels, because DII degradation is induced by auxin. Indeed, *DR5v2*-expressing cells showed low DII-VENUS fluorescence (Figure 1J–1L). Strikingly, MP was expressed in ovule cells that showed DII-VENUS activity, confirming its presence in cells with low auxin levels.

To determine whether MP actively regulates transcription in cells of ovule primordia with low auxin levels, we analyzed the expression of the direct MP target genes *TARGET OF MONOPTEROS 3* (*TMO3*), *TMO5*, *CUP-SHAPED COTYLEDON 1* (*CUC1*) and *CUC2*.[6,10,15] *pTMO3:GFP* was expressed in the proximal region of ovule primordia and in a few cells in the chalaza (Figure 1M). At the same developmental stage, *pTMO5:GFP* expression was also limited to a few cells at the boundary between the chalaza and the nucellus (Figures 1N and 1O). *In situ* hybridization detected *CUC1* and *CUC2* transcripts at the boundaries between ovules,[10] in the chalaza, and in the boundary between the chalaza and the nucellus (Figure 1P–1R). These results show that the expression of *TMO3, TMO5, CUC1* and *CUC2* spatially overlaps with MP-GFP localization and suggests the existence of a mechanism that allows MP to activate its targets at auxin levels that are insufficient to degrade DII-VENUS or activate *DR5v2*.

Alternative Splicing Generates an MP Protein That Lacks a CTD

The dependence of MP function on auxin, similar to that of other ARF transcription factors, is mediated by Aux/IAA protein interaction with the MP C-terminal PB1 domain.[18] We therefore queried whether naturally occurring MP isoforms that lack the MP C-terminal PB1 domain (CTD) exist. We performed an RNA-seq experiment at high-sequencing depth (100 million reads) using wild-type inflorescences (See STAR Methods). In this dataset, we detected reads that mapped to sequences within, or that entirely spanned, intron 11 of the *MP* gene (Figure S1A). The existence of an alternative *MP* isoform that retains only intron 11 (*MP11ir*) was confirmed using RT-PCR (Figure 2A). Expression of *MP11ir* was high in inflorescences and very low in seedlings, whereas no *MP11ir* was detected in leaves. Using a digital PCR approach, the contribution of *MP11ir* to the amount of total *MP* transcript in inflorescences tissues was determined to be 5.9%–6.2% (Figure 2B). Notably, retention of intron 11 leads to a premature stop codon prior to the CTD domain (Figures 2C and S1B).

Intron retention (IR) is the most prevalent AS event in plants;[19,20] however, IR generates mostly non-sense mRNAs that harbor premature terminal codons, which are degraded by the nonsense-mediated mRNA decay (NMD) pathway. Consequently, the alternative transcripts might not necessarily represent biologically functional units. To determine whether *MP11ir* transcripts were translated, their association with ribosomes was investigated by polysome profiling[21] using pre-fertilization inflorescences (Figure 2D). In inflorescences, approximately 70% of total *MP* mRNA was detected in the heavy polysome fraction, suggesting they were actively translated (Figure 2D). Likewise, *MP11ir* was associated with polysomes, albeit at lower levels (40%; Figure 2D). As reported for many other *Arabidopsis* transcription factors,[22,23] our data suggest that *MP11ir* transcripts might escape NMD to produce a functional truncated protein.

Furthermore, analysis of the evolutionary conservation of the genomic sequence of *MP* in several species from the *Arabidopsis* genus and in other Brassicaceae taxa revealed that several introns are well conserved (Figure 2E). In particular, introns 1, 2, and 11 are highly conserved among *Arabidopsis thaliana*, *A. lyrata*, *A. halleri*, *Boechera stricta*, *Capsella grandiflora* and *C. rubella*. Among these three introns, intron 11 is the most consistently conserved among the six species, with a degree of conservation comparable to that in the coding sequences (Figure 2E). The sequence conservation of non-coding regions such as introns suggests that these are important for the correct functioning of the gene.

MP11ir Can Restore Pistil and Ovule Formation in *mp* Mutants

Due to the absence of the CTD, MP11ir might function as a transcriptional activator irrespective of the auxin level. Indeed, it is well established that the CTD is essential for the heterotypic ARF–Aux/IAA interactions that confer auxin dependency to ARF activity; however, the MP DBD alone is sufficient to bind auxin-responsive promoters and to interact with other ARFs.[4,24,25]

We hypothesized that MP11ir might be functionally relevant during the reproductive phase. To verify this hypothesis, we expressed the shorter *MP11ir* isoform from the *MP* promoter (*pMP:MP11ir-GFP*, hereafter *pMP:MP11ir*) in plants carrying the hypomorphic *mpS319* mutation. The *mpS319* mutant has lateral branching defects and forms only a few flowers with aberrant numbers and morphologies of floral organs (Figure S2). In particular, almost all *mpS319* pistils are radialized (Figures S3A and S3B) and do not develop proper placental tissue or rarely form ovule primordia (Figure 3A). Phenotypic analysis showed that in three independent lines, *pMP:MP11ir* complemented several developmental defects of the *mpS319* mutant. These included a general recovery of plant architecture, lateral branching and inflorescence, and flower morphology (Figure S2). In *mpS319 pMP:MP11ir* plants, the percentage of pistils that contained ovules increased to 67% of the total pistils analyzed (Figure S3), and the mean of number of ovules formed per pistil increased significantly (36 ovules ± SE) (Figure 3A).

(D) Polysome profiling from wild-type inflorescences. In (D), blue curves represent the distribution of *MP*, *MP11ir* and *ACT* mRNAs along the sucrose gradient determined by real-time PCR. The amount of mRNA in each of the three fractions (monosomes, light polysomes and heavy polysomes) is expressed as the percentage of the total amount of the mRNA in the microsomes. Red curves refer to EDTA-treated samples, which disrupts polysomes and shifts target profiles toward lighter fractions.

(E) VISTA plots of the evolutionary conservation of the genomic sequence of *MP* in six species: three from the *Arabidopsis* genus (*Arabidopsis thaliana*, *A. lyrata*, *A. halleri*) and three other Brassicaceae species (*Boechera stricta*, *Capsella grandiflora* and *C. rubella*). The plot represents fragments with more than 70% nucleotide sequence conservation. Colors under the lines highlight the function of the depicted region; conserved non-coding sequences (CNS) representing introns 1, 2 and 11 are depicted in pink. See also Figure S1 and Table S1.

Please cite this article in press as: Cucinotta et al., Alternative Splicing Generates a MONOPTEROS Isoform Required for Ovule Development, Current Biology (2020), https://doi.org/10.1016/j.cub.2020.11.026

CellPress
OPEN ACCESS

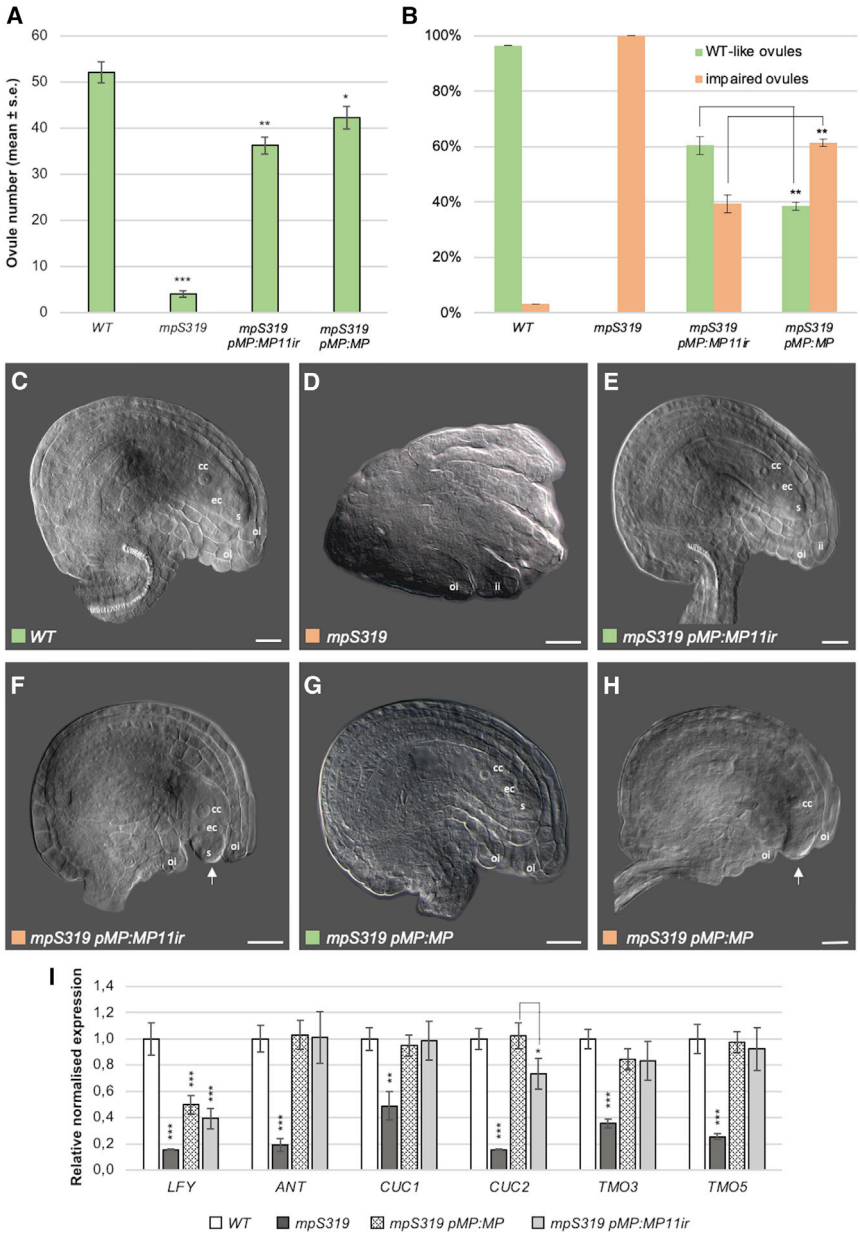

Figure 3. Complementation of Ovule Development in *mpS319 pMP:MP11ir* and *mpS319 pMP:MP*

(A) Ovule number per pistil in wild type, *mpS319, mpS319 pMP:MP11ir* and *mpS319 pMP:MP* lines. $p^{*} < 0.05$; $p^{**} < 0.01$ and $p^{***} < 0.001$ (one-way ANOVA and Tukey's HSD test; n = 3 pistils from five plants of three independent lines).

(B) Percentage of phenotypically wild-type and defective ovules out of the total number of ovules analyzed in wild type, *mpS319 pMP:MP11ir* and *mpS319 pMP:MP* compared to *mpS319* $p^{**} < 0.01$ (one-way ANOVA and Tukey's HSD test; n = 200 ovules from plants of three independent lines).

(C, E, and G) Wild type, *mpS319 pMP:MP11ir* and *mpS319 pMP:MP* ovules with mature gametophytes.

(D) An aberrant *mpS319* ovule, (F–H) exemplary *mpS319 pMP:MP11ir* and *mpS319 pMP:MP* ovules with unsealed integuments at the micropylar region. White arrows indicate the embryo sac protruding from open integuments. Scale bar, 20 μm. (I) Expression analysis of MP direct targets. *LFY* is a floral meristem identity gene, whereas *ANT, CUC1, CUC2, TMO3* and *TMO5* are involved in ovule development. cc, central cell, ec, egg cell; ii, inner integument; oi, outer integument; s, synergid. Error bars indicate the SE based on three biological replicates. $p^{*} < 0.05$; $p^{**} < 0.01$ and $p^{***} < 0.001$ (one-way ANOVA and Tukey's HSD test) and data were normalized with respect to *ACT8-2* and *UBI10* mRNA levels. See also Figures S2 and S3.

At later stages of ovule development, the ovules that rarely formed in *mpS319* had an aberrant morphology, impaired integuments, and aborted embryo sacs (Figures 3B and 3D). In *mpS319 pMP:MP11ir*, 60% of the ovules analyzed displayed a normal development of the integuments that correctly covered the mature gametophyte (Figures 3B and 3E). In the remaining 40% of *mpS319 pMP:MP11ir* ovules, the gametophyte was correctly formed, but the integuments did not properly elongate, causing the embryo to protrude from the micropylar side that remained open (Figures 3B and 3F).

Additionally, we tested the ability of *MP11ir* to complement the strong *arf5.1* mutant allele, which carries a T-DNA insertion in the exon that encodes the DBD. Similar to in the *mpS319* background, *pMP:MP11ir* restored fertility, plant and inflorescence morphology in the *arf5.1* background (Figure S2).

Collectively, the results show that despite being uncoupled from classical auxin regulation due to the absence of the CTD, MP11ir can still perform several native MP functions during ovule development.

A Lack of MP11ir Impacts Correct Ovule Integument Elongation

To test whether the function of the alternative MP11ir isoform was required during the plant reproductive phase, we expressed the canonical intron-less *MP* transcript that cannot be differentially spliced, from the *MP* promoter in the *mpS319* mutant background (hereafter *mpS319 pMP:MP*). Before proceeding with this analysis, we showed by qRT-PCR that the expression level of *MP* in three independent transgenic lines was comparable to that of *MP11ir* (Figure S3C). Phenotypic analysis of *mpS319 pMP:MP* plants showed that defects in lateral branching and inflorescence morphogenesis were complemented by the canonical *MP*, similar to the degree of complementation observed by *MP11ir* (Figure S3). Moreover, in the strong *arf5.1* background, *MP* and *MP11ir* complemented defects in plant architecture and inflorescence morphology to similar extents (Figure S2). The complementation of pistil defects by *MP* was more pronounced than that by *MP11ir*; indeed, in *mpS319 pMP:MP* plants, the percentage of pistils that developed ovules (the total of phenotypically wild-type and partially

Please cite this article in press as: Cucinotta et al., Alternative Splicing Generates a MONOPTEROS Isoform Required for Ovule Development, Current Biology (2020), https://doi.org/10.1016/j.cub.2020.11.026

radialised pistils) reached 91% of the total analyzed pistils, whereas for *mpS319 pMP:MP11ir* plants, this percentage was 68% (Figure S3). This suggests that correct apical–basal and abaxial–adaxial patterning of pistils was more efficiently regulated by full-length MP.

The ability to form ovule primordia in *mpS319 pMP:MP* and *mpS319 pMP:MP11ir* plants did not differ significantly, and the number of ovules was approximately 20% less than that observed in wild-type (Figure 3A). At later stages, we detected phenotypically wild-type ovules, and ovules in which the integuments did not correctly surround and seal the mature gametophyte, in *mpS319 pMP:MP* and *mpS319 pMP:MP11ir* plants (Figures 3G and 3H). However, the percentage of impaired ovules was significantly higher in *mpS319 pMP:MP* plants (61%) than in *mpS319 pMP:MP11ir* plants (39%) and accordingly, the percentage of phenotypically wild-type ovules was higher in *mpS319 pMP:MP11ir* plants (Figure 3B), suggesting that *MP11ir* was more efficient than canonical *MP* in complementing the defects in ovule integument morphology in *mpS319*. These results demonstrate that both *MP* and *MP11ir* complemented the *mpS319* and *arf5.1* phenotype, implying that in the majority of developmental contexts that we analyzed, the CTD domain of MP is not strictly required. A similar conclusion was proposed, based on the observation that an artificially truncated MP protein (MPΔ) lacking the CTD, partially restored flower formation and fertility in the severe *mp-G12* mutant.[26]

The comparison between *mpS319 pMP:MP11ir* and *mpS319 pMP:MP* indicated that the MP11ir isoform was not essential for the complementation of lateral branching, flower and pistil morphogenesis, and ovule primordium formation defects, but was also functional in these contexts. On the contrary, the absence of MP11ir in *mpS319 pMP:MP* plants resulted in a stronger reduction in integument growth than in *mpS319 pMP:MP11ir* plants, suggesting that MP11ir function is tissue- and developmental-specific in ovules.

The inability of either isoforms to fully complement the *mp* mutants suggests that both are required for wild-type development, probably in a spatially and temporally balanced stoichiometry. However, alternatively the constructs we used might miss regulatory elements located in the 5¢ or 3¢ regions of the *MP* locus or in the introns, that were not included in the constructs.

Lastly, we quantified the expression of direct MP targets involved in ovule development. Consistent with the rescue of pistil and ovule formation in *mpS319 pMP:MP11ir* and *mpS319 pMP:MP* plants, the expression levels of *ANT, CUC1, TMO3* and *TMO5* were comparable to those in wild-type (Figure 3I). However, the reduction in the expression of *LFY*, which performs a more general function in floral meristem identity, was not fully recovered in *mpS319 pMP:MP11ir* or *mpS319 pMP:MP* plants (Figure 3I). The expression of *CUC2* was slightly lower in *mpS319 pMP:MP11ir* than in wild type and *mpS319 pMP:MP,* but statistically higher than those in *mpS319* (Figure 3I).

These observations again suggest that the activity of MP is not strictly regulated via its CTD. The importance of truncated ARFs in several plant species has been highlighted previously. For example, the proportion of truncated ARFs is extremely high in *Medicago truncatula* and *Zea mays*.[1,2,27,28] The absence of the CTD does not interfere with the DNA binding-domain (DBD) activity of MP, because the DBD is sufficient to target MP to an auxin-responsive reporter gene in protoplast transfection assays.[4] Furthermore, the absence of the CTD does not impair MP homo-dimerization, since protein structure resolution has shown that MP–MP binding can occur through the DBD.[25] An MP protein that lacks the CTD should still interact with BRAHMA (BRM) to activate key regulators of flower primordium initiation.[6] Moreover, it has been shown that expression of the MP DBD domain alone fused to BUSHY, which acts as a bridge with BRM, could partially complement the *mp* mutant phenotype,[6] again emphasizing that the transcriptional activation role of MP can be uncoupled from auxin regulation. This characteristic of MP is clearly fundamental, since several studies[29,30] have shown that MP is responsible for the correct expression and polar localization of the PIN1 auxin efflux carrier that generates auxin maxima. This means that initially, *PIN1* regulation by MP is intrinsically required to anticipate auxin concentration maxima, which provides a logical explanation why MP is a functional activator in cells with subthreshold auxin concentrations. In conclusion, our observations combined with previous studies, suggest that the current model according to which auxin needs to degrade Aux/IAA to allow MP to activate its target genes during plant development will need revision. Consequently, further efforts will be needed to deeply understand the regulation and activity of ARF transcription factors during reproductive development.

STAR★METHODS

Detailed methods are provided in the online version of this paper and include the following:

- KEY RESOURCES TABLE
- RESOURCE AVAILABILITY
  - Lead Contact
  - Materials Availability
  - Data and Code Availability
- EXPERIMENTAL MODEL AND SUBJECT DETAILS
  - Plant material and growth conditions
- METHOD DETAILS
  - Optical and confocal microscopy
  - *In situ* hybridization
  - AS PCR analysis
  - Droplet digital PCR assay
  - Polysome isolation and fractionation
  - RNA-seq analysis
  - Sequence conservation analysis
- QUANTIFICATION AND STATISTICAL ANALYSIS

SUPPLEMENTAL INFORMATION

Supplemental Information can be found online at https://doi.org/10.1016/j.cub.2020.11.026.

ACKNOWLEDGMENTS

We would like to thank Dr. John Chandler for editing and discussing the manuscript. The authors thank Dr. Francesca Galbiati and Dr. Luca Tadini for technical support. A.C., A.G., and S.M. were supported by the Ministero dell'Istruzione, dell'Università e della Ricerca (MIUR). M.C. was funded by MIUR-PRIN 2012. A.B. was supported by SEXSEED Project H2020-MSCA-RISE-2015.

AUTHOR CONTRIBUTIONS

M.C. and A.C. contributed equally to this work. Conceived and designed the experiments: M.C., A.C., S.B., M.K., and L.C. Performed the experiments: M.C., A.C., A.G., C.A., and S.O. Analyzed the data: M.C., A.C., M.K., and L.C. Performed bioinformatic analysis: S.M. and A.B. Contributed reagents/materials/analysis tools: S.B., D.W., and L.C. Wrote the paper: M.C., A.C., M.K., and L.C.

DECLARATION OF INTERESTS

The authors declare no competing interests.

Received: June 18, 2019
Revised: November 6, 2020
Accepted: November 11, 2020
Published: December 3, 2020

REFERENCES

1. Chandler, J.W. (2016). Auxin response factors. Plant Cell Environ. *39*, 1014–1028.
2. Li, S.B., Xie, Z.Z., Hu, C.G., and Zhang, J.Z. (2016). A Review of Auxin Response Factors (ARFs) in Plants. Front. Plant Sci. *7*, 47.
3. Ulmasov, T., Murfett, J., Hagen, G., and Guilfoyle, T.J. (1997). Aux/IAA proteins repress expression of reporter genes containing natural and highly active synthetic auxin response elements. Plant Cell *9*, 1963–1971.
4. Tiwari, S.B., Hagen, G., and Guilfoyle, T. (2003). The roles of auxin response factor domains in auxin-responsive transcription. Plant Cell *15*, 533–543.
5. Hamann, T., Benkova, E., Bäurle, I., Kientz, M., and Jürgens, G. (2002). The Arabidopsis BODENLOS gene encodes an auxin response protein inhibiting MONOPTEROS-mediated embryo patterning. Genes Dev. *16*, 1610–1615.
6. Wu, M.F., Yamaguchi, N., Xiao, J., Bargmann, B., Estelle, M., Sang, Y., and Wagner, D. (2015). Auxin-regulated chromatin switch directs acquisition of flower primordium founder fate. eLife *4*, e09269.
7. Berleth, T., and Jürgens, G. (1993). The role of the monopteros gene in organising the basal body region of the Arabidopsis embryos. Trends Genet. *9*, 299.
8. De Smet, I., Lau, S., Voss, U., Vanneste, S., Benjamins, R., Rademacher, E.H., Schlereth, A., De Rybel, B., Vassileva, V., Grunewald, W., et al. (2010). Bimodular auxin response controls organogenesis in Arabidopsis. Proc. Natl. Acad. Sci. USA *107*, 2705–2710.
9. Donner, T.J., Sherr, I., and Scarpella, E. (2009). Regulation of preprocambial cell state acquisition by auxin signaling in Arabidopsis leaves. Development *136*, 3235–3246.
10. Galbiati, F., Sinha Roy, D., Simonini, S., Cucinotta, M., Ceccato, L., Cuesta, C., Simaskova, M., Benková, E., Kamiuchi, Y., Aida, M., et al. (2013). An integrative model of the control of ovule primordia formation. Plant J. *76*, 446–455.
11. Hardtke, C.S., and Berleth, T. (1998). The Arabidopsis gene MONOPTEROS encodes a transcription factor mediating embryo axis formation and vascular development. EMBO J. *17*, 1405–1411.
12. Przemeck, G.K., Mattsson, J., Hardtke, C.S., Sung, Z.R., and Berleth, T. (1996). Studies on the role of the Arabidopsis gene MONOPTEROS in vascular development and plant cell axialization. Planta *200*, 229–237.
13. Weijers, D., Schlereth, A., Ehrismann, J.S., Schwank, G., Kientz, M., and Jürgens, G. (2006). Auxin triggers transient local signaling for cell specification in Arabidopsis embryogenesis. Dev. Cell *10*, 265–270.
14. Yamaguchi, N., Wu, M.-F., Winter, C.M., Berns, M.C., Nole-Wilson, S., Yamaguchi, A., Coupland, G., Krizek, B.A., and Wagner, D. (2013). A molecular framework for auxin-mediated initiation of flower primordia. Dev. Cell *24*, 271–282.
15. Schlereth, A., Möller, B., Liu, W., Kientz, M., Flipse, J., Rademacher, E.H., Schmid, M., Jürgens, G., and Weijers, D. (2010). MONOPTEROS controls embryonic root initiation by regulating a mobile transcription factor. Nature *464*, 913–916.
16. Brunoud, G., Wells, D.M., Oliva, M., Larrieu, A., Mirabet, V., Burrow, A.H., Beeckman, T., Kepinski, S., Traas, J., Bennett, M.J., and Vernoux, T. (2012). A novel sensor to map auxin response and distribution at high spatio-temporal resolution. Nature *482*, 103–106.
17. Liao, C.-Y., Smet, W., Brunoud, G., Yoshida, S., Vernoux, T., and Weijers, D. (2015). Reporters for sensitive and quantitative measurement of auxin response. Nat. Methods *12*, 207–210, 2, 210.
18. Vernoux, T., Brunoud, G., Farcot, E., Morin, V., Van den Daele, H., Legrand, J., Oliva, M., Das, P., Larrieu, A., Wells, D., et al. (2011). The auxin signalling network translates dynamic input into robust patterning at the shoot apex. Mol. Syst. Biol. *7*, 508.
19. Jia, J., Long, Y., Zhang, H., Li, Z., Liu, Z., Zhao, Y., Lu, D., Jin, X., Deng, X., Xia, R., et al. (2020). Post-transcriptional splicing of nascent RNA contributes to widespread intron retention in plants. Nat. Plants *6*, 780–788.
20. Ner-Gaon, H., Halachmi, R., Savaldi-Goldstein, S., Rubin, E., Ophir, R., and Fluhr, R. (2004). Intron retention is a major phenomenon in alternative splicing in Arabidopsis. Plant J. *39*, 877–885.
21. Oliveto, S., Alfieri, R., Miluzio, A., Scagliola, A., Secli, R.S., Gasparini, P., Grosso, S., Cascione, L., Mutti, L., and Biffo, S. (2018). A polysome-based microrna screen identifies miR-24-3p as a novel promigratory mirna in mesothelioma. Cancer Res. *78*, 5741–5753.
22. Chaudhary, S., Jabre, I., Reddy, A.S.N., Staiger, D., and Syed, N.H. (2019). Perspective on alternative splicing and proteome complexity in plants. Trends Plant Sci. *24*, 496–506.
23. Kalyna, M., Simpson, C.G., Syed, N.H., Lewandowska, D., Marquez, Y., Kusenda, B., Marshall, J., Fuller, J., Cardle, L., McNicol, J., et al. (2012). Alternative splicing and nonsense-mediated decay modulate expression of important regulatory genes in Arabidopsis. Nucleic Acids Res. *40*, 2454–2469.
24. Krogan, N.T., and Berleth, T. (2012). A dominant mutation reveals asymmetry in MP/ARF5 function along the adaxial-abaxial axis of shoot lateral organs. Plant Signal. Behav. *7*, 940–943.
25. Boer, D.R., Freire-Rios, A., van den Berg, W.A., Saaki, T., Manfield, I.W., Kepinski, S., López-Vidrieo, I., Franco-Zorrilla, J.M., de Vries, S.C., Solano, R., et al. (2014). Structural basis for DNA binding specificity by the auxin-dependent ARF transcription factors. Cell *156*, 577–589.
26. Krogan, N.T., Ckurshumova, W., Marcos, D., Caragea, A.E., and Berleth, T. (2012). Deletion of MP/ARF5 domains III and IV reveals a requirement for Aux/IAA regulation in Arabidopsis leaf vascular patterning. New Phytol. *194*, 391–401.
27. Shen, C., Yue, R., Sun, T., Zhang, L., Xu, L., Tie, S., Wang, H., and Yang, Y. (2015). Genome-wide identification and expression analysis of auxin response factor gene family in Medicago truncatula. Front. Plant Sci. *6*, 73.
28. Finet, C., Berne-Dedieu, A., Scutt, C.P., and Marlétaz, F. (2013). Evolution of the ARF gene family in land plants: old domains, new tricks. Mol. Biol. Evol. *30*, 45–56.
29. Wenzel, C.L., Schuetz, M., Yu, Q., and Mattsson, J. (2007). Dynamics of MONOPTEROS and PIN-FORMED1 expression during leaf vein pattern formation in Arabidopsis thaliana. Plant J. *49*, 387–398.
30. Bhatia, N., Bozorg, B., Larsson, A., Ohno, C., Jönsson, H., and Heisler, M.G. (2016). Auxin acts through MONOPTEROS to regulate plant cell polarity and pattern phyllotaxis. Curr. Biol. *26*, 3202–3208.
31. Cole, M., Chandler, J., Weijers, D., Jacobs, B., Comelli, P., and Werr, W. (2009). DORNROSCHEN is a direct target of the auxin response factor MONOPTEROS in the Arabidopsis embryo. Development *136*, 1643–1651.
32. Okushima, Y., Overvoorde, P.J., Arima, K., Alonso, J.M., Chan, A., Chang, C., Ecker, J.R., Hughes, B., Lui, A., Nguyen, D., et al. (2005). Functional genomic analysis of the AUXIN RESPONSE FACTOR gene family

members in Arabidopsis thaliana: unique and overlapping functions of ARF7 and ARF19. Plant Cell *17*, 444–463.

33. Aronesty, E. (2013). Comparison of sequencing utility programs. Open Bioinforma. J. *7*, 1–8.
34. Dobin, A., Davis, C.A., Schlesinger, F., Drenkow, J., Zaleski, C., Jha, S., Batut, P., Chaisson, M., and Gingeras, T.R. (2013). STAR: ultrafast universal RNA-seq aligner. Bioinformatics *29*, 15–21.
35. Robinson, J.T., Thorvaldsdóttir, H., Winckler, W., Guttman, M., Lander, E.S., Getz, G., and Mesirov, J.P. (2011). Integrative genomics viewer. Nat. Biotechnol. *29*, 24–26.
36. Buels, R., Yao, E., Diesh, C.M., Hayes, R.D., Munoz-Torres, M., Helt, G., Goodstein, D.M., Elsik, C.G., Lewis, S.E., Stein, L., and Holmes, I.H. (2016). JBrowse: a dynamic web platform for genome visualization and analysis. Genome Biol. *17*, 66.
37. Dibitetto, D., La Monica, M., Ferrari, M., Marini, F., and Pellicioli, A. (2018). Formation and nucleolytic processing of Cas9-induced DNA breaks in human cells quantified by droplet digital PCR. DNA Repair (Amst.) *68*, 68–74.
38. Mustroph, A., Juntawong, P., and Bailey-Serres, J. (2009). Isolation of plant polysomal mRNA by differential centrifugation and ribosome immunopurification methods. Methods Mol. Biol. *553*, 109–126.

Please cite this article in press as: Cucinotta et al., Alternative Splicing Generates a MONOPTEROS Isoform Required for Ovule Development, Current Biology (2020), https://doi.org/10.1016/j.cub.2020.11.026

CellPress
OPEN ACCESS

STAR★METHODS

KEY RESOURCES TABLE

REAGENT or RESOURCE	SOURCE	IDENTIFIER
Bacterial and Virus Strains		
Escherichia coli DH5α	N/A	N/A
Agrobacterium tumefaciens GV3101	N/A	N/A
Chemicals, Peptides, and Recombinant Proteins		
Q5 High-Fidelity DNA Polymerase	NEB	Cat#M0491S
Basta Herbicide	BASF	N/A
GoTaq DNA Polymerase	Promega	Cat#M3001
Critical Commercial Assays		
NucleoSpin RNA Plant kit	Macherey-Nagel	Cat#740949.50
TURBO™ DNase	ThermoFisher Scientific	Cat#AM2238
ddPCR™ Supermix for Probes	Bio-Rad	Cat#186-3023
ImProm-II™ Reverse Transcription System	Promega	Cat#A3800
SuperScript™ IV VILO™ Master Mix with ezDNase™	ThermoFisher Scientific	Cat#11766050
iTaq SYBR green master mix	Bio-Rad	Cat#1725121
Cstm ddPCR FAM Assay 200R	Bio-Rad	Cat#10031276
Cstm ddPCR HEX Assay 200R	Bio-Rad	Cat#10031279
DIG RNA Labeling Kit (SP6/T7)	Roche	Cat#11175025910
Deposited Data		
RNA-seq *Arabidopsis thaliana* Col-0 inflorescences	this study	NCBI Database: SRR12990564, https://www.ncbi.nlm.nih.gov/sra/SRR12990564N
Experimental Models: Organisms/Strains		
Arabidopsis thaliana pTMO3::3xGFP	[15]	N/A
Arabidopsis thaliana DRv2::ntdTomato	[17]	N/A
Arabidopsis thaliana mpS319	[31]	N/A
Arabidopsis thaliana arf5-1	[32]	N/A
Arabidopsis thaliana DII-VENUS	[16]	N/A
Arabidopsis thaliana pMP:MP11ir-GFP	this study	N/A
Arabidopsis thaliana pMP:MP	this study	N/A
Arabidopsis thaliana Col-0	The Nottingham *Arabidopsis* Stock Centre (NASC)	N/A
Arabidopsis thaliana pMP:MP-GFP	[15]	N/A
Arabidopsis thaliana pTMO5::3xGFP	[15]	N/A
Oligonucleotides		
Oligonucleotides for cloning and for expression analysis	see Table S1	N/A
Oligonucletides for detection of alternative splicing	see Table S1	N/A
Recombinant DNA		
Plasmid: pMP:MP11ir-GFP	this study	N/A
Software and Algorithms		
LAS AF 2.2.0	Leica Microsystems Srl	https://www.leica-microsystems.com/
QuantaSoft™	Bio-Rad	https://www.bio-rad.com/en-it/SearchResults?Text=quantasoft

(*Continued on next page*)

Please cite this article in press as: Cucinotta et al., Alternative Splicing Generates a MONOPTEROS Isoform Required for Ovule Development, Current Biology (2020), https://doi.org/10.1016/j.cub.2020.11.026

Continued

REAGENT or RESOURCE	SOURCE	IDENTIFIER
BioLogic LP software	Bio-Rad	https://www.bio-rad.com/en-it/product/lp-data-view-software-for-biologic-lp-system
Fastq-mcf (Ea-utils package)	[33]	N/A
STAR software	[34]	https://github.com/alexdobin/STAR
IGV software	[35]	https://software.broadinstitute.org/software/igv/download
JBrowse	[36]	https://jbrowse.org/jb2/
Axiovision 4.1	Carl Zeiss AG	https://www.micro-shop.zeiss.com/it/ch/

RESOURCE AVAILABILITY

Lead Contact

Further information and requests for resources should be directed to and will be fulfilled by the Lead Contact, Lucia Colombo (lucia.colombo@unimi.it).

Materials Availability

This study did not generate new unique reagents.

Data and Code Availability

The accession number for the Arabidopsis Col-0 inflorescences RNA-sequencing data AT_COL0_INF1_UNIMI reported in this paper is NCBI Database: SRR12990564, https://www.ncbi.nlm.nih.gov/sra/SRR12990564.)

EXPERIMENTAL MODEL AND SUBJECT DETAILS

Plant material and growth conditions

Plants were grown in the greenhouse at 22°C under long-day (16 h light/8 h dark) conditions. *pMP:MP-GFP*, *pTMO5::3 × GFP*, *pTMO3::3 × GFP*[15] and *DR5v2::ntdTomato*[17] were provided by Prof. Dolf Weijers. The mutants *mpS319*,[31] *arf5.1* (SALK_023812)[32] and the *DII-VENUS* reporter[16] have been described previously. To construct *pMP:MP11ir-GFP*, the *MP* genomic locus was amplified from −5,033 to +3,379 with respect to the start codon and cloned into pGreenII to obtain *MP11ir* fused to *GFP*. To construct *pMP:MP(cDNA):tMP*, −4,107 bp of *MP* promoter sequence were ligated with 902 bp of *MPcds* and 178 bp of *MP* 3¢UTR in pPLV cloning vector. The obtained plasmids were then introgressed into *mpS319* and *arf5.1* background.

METHOD DETAILS

Optical and confocal microscopy

Images of inflorescences and pistils were taken with a Zeiss® Axiocam MRc5 camera and a Leica® MZ6 stereomicroscope and were processed using Axiovision (version 4.1) software. For confocal laser scanning microscopy, dissected pistils were mounted in water and observed with an SP2 Leica confocal microscope. eGFP was excited at 488 nm and detected at 498–530 nm, tdTomato was excited at 561 nm and detected at 571–630 nm. We used a 40 × water-immersion objective (numerical aperture = 1.25, pinhole), confocal scans were performed with the pinhole at 1 airy unit. Images were collected in multi-channel mode, and overlay images were generated using Leica analysis software LAS AF 2.2.0.

In situ hybridization

In situ hybridizations were performed as previously described.[10] Digoxygenin-labeled antisense RNA probes were generated by *in vitro* transcription with the DIG RNA Labeling Kit (SP6/T7) by Roche. Developing inflorescences of wild-type *Arabidopsis* plants were fixed and embedded in Paraplast Plus embedding medium; sections were hybridized and then mounted with a coverslip and subsequently observed using a Zeiss Axiophot D1 microscope equipped with differential interface contrast (DIC) optics.

AS PCR analysis

RNA was extracted using the NucleoSpin RNA Plant kit (Macherey-Nagel®), treated with Thermo Fisher Scientific® TURBO DNase and subsequently reverse-transcribed using the Promega® ImProm-II Reverse Transcription System. The synthesized cDNA was used for PCR with *ACTIN* as a control to exclude DNA contamination. PCR for AS detection was performed using primer pairs specific to intron 11 and the exon 11–exon 12 junction. Primers are listed in Table S1.

Please cite this article in press as: Cucinotta et al., Alternative Splicing Generates a MONOPTEROS Isoform Required for Ovule Development, Current Biology (2020), https://doi.org/10.1016/j.cub.2020.11.026

Droplet digital PCR assay

ddPCR was performed as in[37] using a Bio-rad QX200 Droplet Digital PCR System according to the suppliers instructions and with all required reagents and disposables from Bio-rad. The ddPCR reaction mix contained 2 μL cDNA (150 ng), 10 μL 2 × ddPCR Supermix for Probes (no dUTP), 1 μL 20 × HEX/FAM assay and dH_2O to a volume of 20 μL per sample. Universal DG8 cartridge, Droplet generation oil for probes and DG8 gaskets were required for droplet formation into the droplet generator (QX200). Then, 40 μL droplet emulsion was transferred to a 96-well ddPCR plate (BioRad) and sealed with a PX1 machine. PCR was performed using the following program: 95°C for 5 min; 39 cycles of 95°C for 30 s and 60°C for 1 min; 98°C for 10 min then the temperature was held at 12°C. Finally, FAM and HEX fluorescence was read in the droplet reader QX200 using QuantaSoft software. The number of copies/μL of each target locus was determined by setting an identical empirical baseline threshold for all samples. Primers and probes are listed in Table S1.

Polysome isolation and fractionation

The total polysome fraction was prepared as previously described[38] with minor modification. Fractionation and RNA extraction were performed as in.[21] To distinguish miRNAs that sedimented with heavy polysomes but were not physically bound to them, we disrupted polysomes by adding 30 mmol L^{-1} EDTA after lysate preparation. Equal amounts of RNA were loaded onto a 15%–50% sucrose gradient with or without 10 mmol L^{-1} EDTA, and centrifuged at 39,000 rpm for 3 h in a SW41Ti Beckman rotor at 4°C. The gradient was then analyzed by continuous flow absorbance at 254 nm, recorded by BioLogic LP software (Bio-Rad), and fractions were collected and kept on ice to avoid RNA degradation. The following fractions were collected: (i) monosome pool, from the top of the gradient to the 80S peak; (ii) light polysomes and (iii) heavy polysomes. Samples were incubated with proteinase K and 1% SDS for 1 h at 37°C. RNA was extracted with phenol/chloroform/isoamyl alcohol and quantified with Nanodrop and Qubit. The same amount of RNA from each fraction was DNase-treated and reverse-transcribed with SuperScript IV VILO Master Mix with ezDNase Enzyme (Invitrogen). The distribution of mRNAs among the three fractions was determined by real-time PCR using a CFX96 Detection System with Bio-Rad iTaq SYBR green master mix. RT-PCR primers are listed in Table S1. The amount of a speciðc mRNA in each of the three fractions was expressed as a percentage of the total amount of mRNA in the translational machinery.

RNA-seq analysis

RNA was extracted from wild-type Col-0 pre-fertilization inflorescences using the NucleoSpin RNA Plant kit (Macherey-Nagel®). RNA-Seq libraries were prepared and sequenced at Novogene (https://en.novogene.com/) following the manufacturer's instructions. The library insert size was approximately 300 bp. The DNA was sequenced in an Illumina HiSeq4000 system as 2 × 150-bp pair ends. The data reads (100 millions) were processed using Fastq-mcf from the Ea-utils[33] package. The reads were mapped to the *Arabidopsis* genome version TAIR10 with STAR[34] using the default parameters. The BAM files were uploaded in IGV[35] with the *Arabidopsis* genome annotation Araport11. A representation of the coverage was depicted with Keynote.

Sequence conservation analysis

The *MONOPTEROS* gene was retrieved from the Phytozome database (accessed on 2019-02-25) using the Locus ID (AT1G19850.1) and then visualized in JBrowser.[36] The VISTA tracks were enabled for all species and each track was manually sorted according to its phylogenetic distance from *Arabidopsis*. The conservation percentage for the colored regions were 70% (blue for exons and red for introns) with a box size of 50 bp.

QUANTIFICATION AND STATISTICAL ANALYSIS

Statistical analysis was implemented using EXCEL. One-way ANOVAs with post hoc Turkey test was carried out by online tool https://astatsa.com/OneWay_Anova_with_TukeyHSD/. Details of statistical tests are provided in figure legends.